Combustion synthesis and properties of fine particle fluorescent aluminous oxides†

J J KINGSLEY, N MANICKAM†† and K C PATIL*

Department of Inorganic and Physical Chemistry, and ††Department of Physics, Indian Institute of Science, Bangalore 560 012, India

Abstract. Fine particle fluorescent aluminous oxide materials like Cr^{3+}-doped α-Al_2O_3 (ruby), $MgAl_2O_4$, $LaAlO_3$, $Y_3Al_5O_{12}$ and Ce^{3+}-doped $Y_3Al_5O_{12}$, $LaMgAl_{11}O_{19}$, $CaAl_{12}O_{19}$ and $CeMgAl_{11}O_{19}$ have been prepared by the combustion of the corresponding metal nitrate–aluminium nitrate–urea/carbohydrazide mixtures at 500°C in less than 5 min. Formation of these Cr^{3+}- and Ce^{3+}-doped aluminous oxides has been confirmed by their characteristic XRD, colour, UV-visible and fluorescence spectra as well as decay time measurements. Ruby (Cr^{3+}/α-Al_2O_3) powder showed characteristic excitation bands at 406 and 548 nm and emission band at 695 nm with the decay time of 3·6 ms.

Keywords. Ruby powder; combustion synthesis; urea; carbohydrazide; aluminium nitrate; metal nitrates; lasers; TV phosphors; fluorescent aluminous oxides.

1. Introduction

Transition metal or rare earth element-doped aluminous oxides are of technological importance due to their applications as lasers (Cr^{3+}/α-Al_2O_3, ruby; $Cr^{3+}/LaAlO_3$, $Nd^{3+}/Y_3Al_5O_{12}$, Nd:YAG) (Geusic *et al* 1966; Cokayne 1972; Hannay 1973), TV phosphors and in fluorescent lamps ($Ce^{3+}/CaAl_{12}O_{19}$) (Scholten and Eijnthoven 1985; Wolfe 1978). These oxides need to be fine particles for use in TV screens and lamps. Recently it was proposed that sub-micron size particles can exhibit optical bistability in the scattering and absorption of light (Leunng 1986). Hence, fine particles of Cr^{3+} doped α-Al_2O_3 (ruby) may be used for ultrafine lasers and ultrafine optical devices (Hirai *et al* 1987).

The conventional method of preparing these transition metal or rare earth-doped aluminous oxide powders is the ceramic method involving the solid state reactions of metal nitrate–urea mixtures (Kingsley *et al* 1988, 1990; Kingsley and Patil 1988). Cr_2O_3–Al_2O_3 (1350°C, 96 h) (De Biasi and Rodrigues 1981), Cr_2O_3–$MgAl_2O_4$ (1250°C, 10 h) (Gillen and Salomon 1970). Fine particles of these doped oxides have been prepared by the sol–gel process e.g. ruby (Hirai *et al* 1987), which is also quite involved and expensive.

Recently, a novel combustion process has been developed for the instant synthesis of fine particle α-alumina and related oxides employing aqueous solutions of metal nitrate–urea mixtures (Kingsley *et al* 1988, 1990; Kingsley and Patil 1988). It was therefore, considered feasible to employ the combustion process to incorporate desired concentrations of impurity ions like Cr^{3+} or Ce^{3+} and prepare fine particle fluorescent aluminous oxide materials such as Cr^{3+}-doped α-Al_2O_3 (ruby), $MgAl_2O_4$, $LaAlO_3$, $Y_3Al_5O_{12}$, Ce^{3+}-doped $Y_3Al_5O_{12}$, $CaAl_{12}O_{19}$, $LaMgAl_{11}O_{19}$ and $CeMgAl_{11}O_{19}$. The results of these investigations are presented in this paper.

---

2. Experimental

Cr^{3+}- and Ce^{3+}-doped aluminous oxides such as Cr^{3+}/Al_2O_3, $MgAl_2O_4$, $LaAlO_3$ and YAG; Ce^{3+}/YAG, $CaAl_{12}O_{19}$ and $LaMgAl_{11}O_{19}$ were prepared by the combustion of mixtures containing the corresponding metal nitrate–aluminium nitrate–urea/carbohydrazide mixtures with the desired concentrations of the dopant ions.

Actual compositions used for the combustion synthesis of Cr^{3+} and Ce^{3+} doped aluminous oxides are given in table 1. The stoichiometric compositions of the mixtures were calculated using the O/F ratio used for the preparation of the host lattices described earlier (Kingsley and Patil 1988; Kingsley *et al* 1988, 1990) except for the addition of dopant ions in the form of respective metal nitrates. The concentrations of the dopant ions are given in terms of weight percentages e.g. 0·05% Cr^{3+}/α-Al_2O_3 implies 0·05 g of Cr_2O_3 in 100 g α-Al_2O_3.

The preparations of 0·5% Cr^{3+}/Al_2O_3 (ruby powder) and 0·05% Ce^{3+}/YAG have been described below as representative for all fluorescent aluminous oxides.

2.1 *Combustion synthesis of fine particle ruby powder (0·5% Cr^{3+}/α-Al_2O_3)*

$Al(NO_3)_3 \cdot 9H_2O$ (20 g) and urea (8 g) are dissolved in a minimum quantity of water along with $Cr(NO_3)_3 \cdot 6H_2O$ (0·07 lg) (corresponding to 0·5% Cr^{3+}/α-Al_2O_3, i.e. 0·5 g Cr_2O_3 for 100 g α-Al_2O_3) in a cylindrical pyrex dish (100 mm dia × 50 mm height) of approximately 300 ml capacity. The dish containing the solution is

Table 1. Compositions of the combustion mixtures.

Compositions of the combustion mixtures*			Fluorescent oxide (colour)
A + $Cr(NO_3)_3$ (0·007 g)		+ urea (8·0 g)	0·05% Cr^{3+}/Al_2O_3 (pink)
A + $Mg(NO_3)_2 \cdot 6H_2O$ (6·83 g)	+ $Cr(NO_3)_3 \cdot 6H_2O$ (0·007 g)	+ urea (10·7 g)	0·05% $Cr^{3+}/MgAl_2O_4$ (pink)
A + $La(NO_3)_3 \cdot 6H_2O$ (23·08 g)	+ $Cr(NO_3)_3 \cdot 6H_2O$ (0·007 g)	+ urea (16·0 g)	0·05% $Cr^{3+}/LaAlO_3$ (pink)
A + $La(NO_3)_3 \cdot 6H_2O$ (23·08 g)	+ $Cr(NO_3)_3 \cdot 6H_2O$ (0·007 g)	+ carbohydrazide (14·4 g)	0·05% $Cr^{3+}/LaAlO_3$ (pink)
A + $Y(NO_3)_3 \cdot 6H_2O$ (12·252 g)	+ $Ce(NO_3)_3 \cdot 6H_2O$ (0·0084 g)	+ urea (12·8 g)	0·05% $Ce^{3+}/Y_3Al_5O_{12}$ (pale yellow)
A + $Y(NO_3)_3 \cdot 6H_2O$ (12·252 g)	+ $Ce(NO_3)_3 \cdot 6H_2O$ (0·0084 g)	+ carbohydrazide (11·52 g)	0·05% $Ce^{3+}/Y_3Al_5O_{12}$ (pale yellow)
A + $Ca(NO_3)_2 \cdot 4H_2O$ (1·05 g)	+ $Ce(NO_3)_3 \cdot 6H_2O$ (0·01 g)	+ urea (8·45 g)	0·14% $Ce^{3+}/CaAl_{12}O_{19}$ (yellow)
A + $Mg(NO_3)_2 \cdot 6H_2O$ (1·24 g)	+ $Ce(NO_3)_3 \cdot 6H_2O$ (2·18 g)	+ urea (9·22 g)	$CeMgAl_{11}O_{19}$ (yellow)
A + $La(NO_3)_3 \cdot 6H_2O$ (2·098 g) + $Ce(NO_3)_3 \cdot 6H_2O$ (0·01 g)	+ $Mg(NO_3)_2 \cdot 6H_2O$ (1·242 g)	+ urea (9·2 g)	0·14% $Ce^{3+}/$ $LaMgAl_{11}O_{19}$ (yellow)

*A = $Al(NO_3)_3 \cdot 9H_2O$ (20 g).

introduced into a muffle furnace ($l = 28$ cm, $b = 17$ cm and $h = 9$ cm) maintained at $500 \pm 10°C$. The mixture undergoes combustion for ~ 2 min and gives a light pink-coloured voluminous and foamy powder (weight 2·72 g, 100% yield) occupying the entire volume of the dish.

2.2 *Combustion synthesis of 0·05% Ce^{3+}-doped $Y_3Al_5O_{12}$ (YAG)*

$Al(NO_3)_3 \cdot 9H_2O$ (20 g), $Y(NO_3)_3 \cdot 6H_2O$ (12·252 g) and carbohydrazide (11·52 g) are dissolved in a minimum quantity of water along with $Ce(NO_3)_3 \cdot 6H_2O$(0·0084 g), (corresponding to 0·05% $Ce^{3+}/Y_3AL_5O_{12}$, i.e. 0·05 g Ce_2O_3 in 100 g $Y_3Al_5O_{12}$) in a cylindrical pyrex dish (100 mm dia × 50 mm height) of 300 ml capacity. The dish is heated at 500°C for <5 min in a muffle furnace as described above and gives a voluminous, pale yellow-coloured foam after combustion.

2.3 *Physical measurements*

The solid combustion products were characterized by powder X-ray diffraction patterns to confirm the formation of host lattices using a Philips X-ray diffractometer model PW 1050/70 using CuKα radiation with Ni filter. The presence of impurity ions in these host lattices was confirmed by their characteristic colours, UV-vis diffuse reflectance spectra, fluorescence spectra as well as decay time measurements. Reflectance spectra were recorded using a Shimadzu UV-vis spectrophotometer model UV-240 with $BaSO_4$ as standard. Fluorescence spectra were obtained using a Hitachi 650–60 fluorescence spectrophotometer as well as the decay time measurements.

Fluorescence decay times were measured using a pulsed laser decay time measurement unit indigenously fabricated. A schematic block diagram of the experimental arrangement is shown in figure 1.

In this, a pulsed nitrogen laser (150 KW, 8 ns and 10 pps), emitting at 337 nm, pumps a dye laser (20 KW, 4 ns and 10 pps), which emits at 409 nm. The dye used is 2,5-diphenyl oxazole dissolved in toluene (10^{-4} M). The dye laser beam is focussed on to a powder sample which is mounted on a sample holder with a quartz window. The fluorescence of the sample collected at 90° is focussed on the slit of a monochromator (Jobin Yuon). The output of the monochromator is focussed on a photo multiplier tube (EMI 9558B). The signals from the photo multiplier tube are fed to a storage oscilloscope (Iiwatsu DMS 6430). The data are collected from the storage oscilloscope by a computer (HP 4207) to which the storage oscilloscope is interfaced. The stored data are processed to obtain the decay curve, ln (intensity) *vs* time plot and the decay times.

3. Results

Combustion synthesized Cr^{3+}- and Ce^{3+}-doped aluminous oxides showed X-ray diffraction patterns similar to those of the parent lattices like α-Al_2O_3, $Y_3Al_5O_{12}$ etc. Typical XRD patterns of Cr^{3+}/Al_2O_3 (ruby powder), $Cr^{3+}/MgAl_2O_4$ and $Ce^{3+}/Y_3Al_5O_{12}$ are shown in figure 2. The lattice parameters calculated from these patterns are in good agreement with the literature values (Powder diffraction file
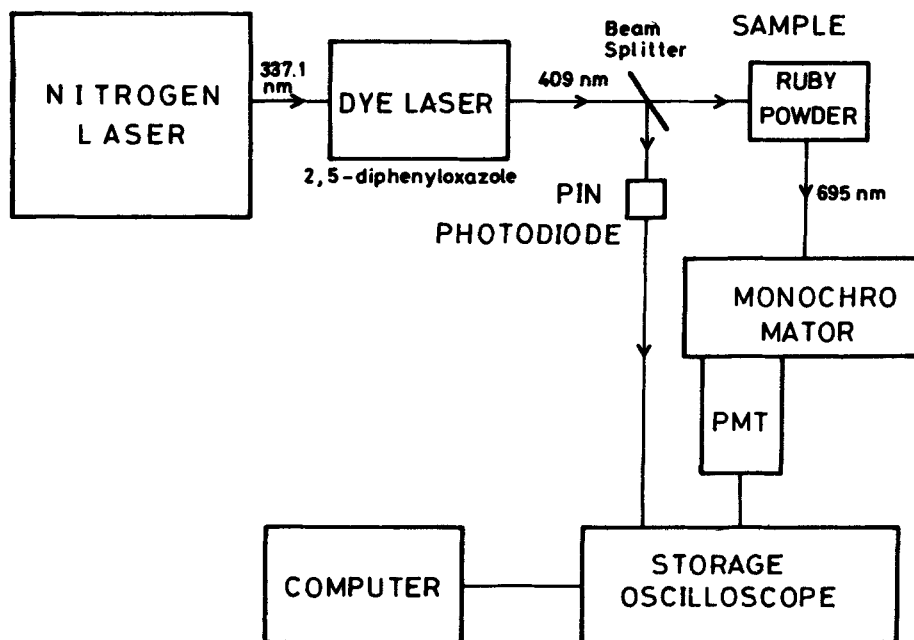
Figure 1. Schematic block diagram of pulsed laser decay time measurement unit.

1967). The calculated (reported) values for these oxides are as follows: (a) α-Al$_2$O$_3$ $a = b = 4.7719$ Å (4.758 Å) and $c = 13.0426$ Å (12.991 Å); (b) MgAl$_2$O$_4$ $a = 8.1153$ Å (8.080 Å); (c) Y$_3$Al$_5$O$_{12}$ $a = 11.987$ Å (12.010 Å). The presence of dopant ions in the host lattices was confirmed by their fluorescence spectra and characteristic colour (e.g. Cr^{3+}/α-Al$_2$O$_3$–pink; Ce^{3+}/Y$_3$Al$_5$O$_{12}$–yellow). These data have been summarized in table 2.

3.1 *Properties of Cr^{3+}/Al$_2$O$_3$ (ruby) powder*

Doping of aluminous oxides with Cr^{3+} ions involves atomic level substitution of the Al^{3+} ions present in these lattices by Cr^{3+} ions. Such substitutions invariably require high temperatures (> 1300°C) and long time periods. For example, formation of ruby (Cr^{3+}-doped α-Al$_2$O$_3$) is known to take place when a Cr$_2$O$_3$–Al$_2$O$_3$ mixture is heated at ± 1350°C for 96 h (De Biasi and Rodrigues 1981). It is gratifying that when a mixture containing Al(NO$_3$)$_3$·9H$_2$O (20 g), Cr(NO$_3$)$_3$·6H$_2$O (0.0148 g) and urea (8 g) was used for the combustion at 500°C, a light pink foamy powder was obtained. It was identified to be ruby (Cr^{3+}-ion doped α-Al$_2$O$_3$) by its characteristic fluorescence spectra (Hirai *et al* 1987) (figure 3), UV-vis spectra (figure 4), decay time measurements (figure 5) and ESR spectrum (figure 6). Figure 3a shows the excitation spectrum of this as prepared from 0.05% Cr^{3+}/Al$_2$O$_3$ powder and figure 3b shows the emission spectrum of the same. The characteristic emission band (Hirai *et al* 1987) (figure 3b), observed at 695 nm by exciting the ruby powder at 548 nm unequivocally proves the formation of ruby. That is, Cr^{3+}-ions have replaced Al^{3+} ions at the 'O_h' sites in the α-Al$_2$O$_3$ lattice. This characteristic emission band is attributed to the transition $^2E_{2g} \rightarrow \, ^4A_{2g}$ of the Cr^{3+}

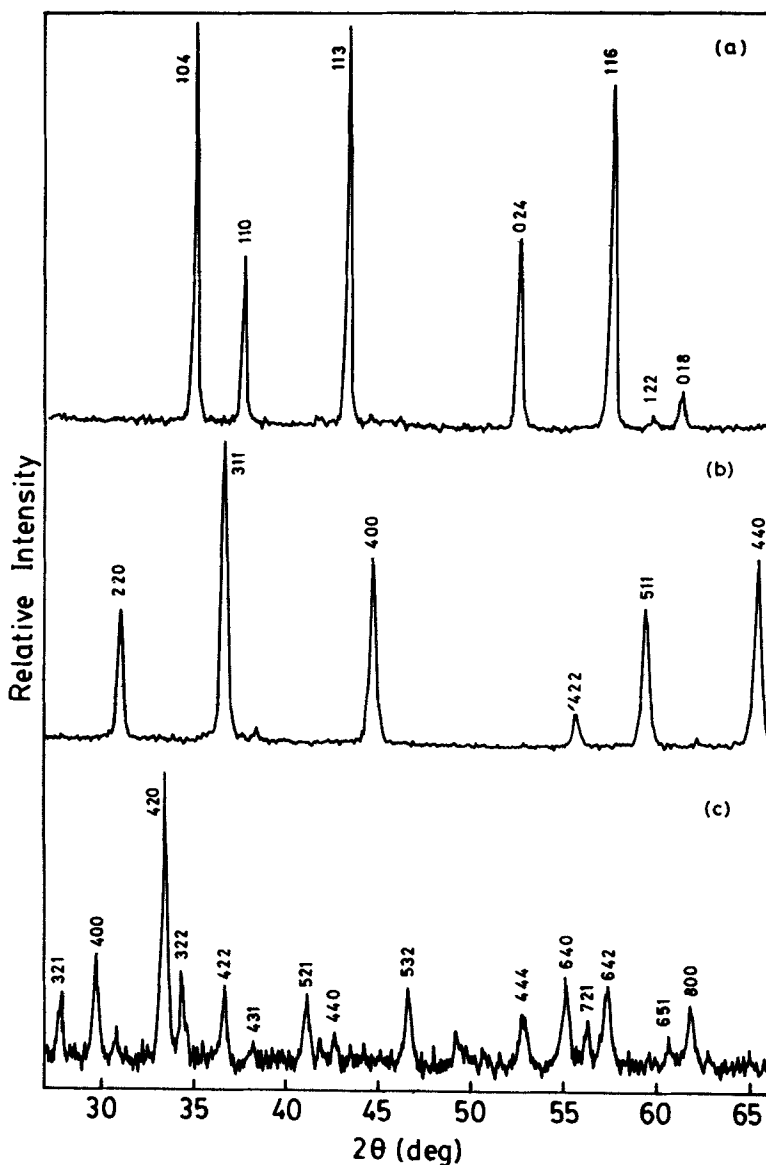**Figure 2.** X-ray powder diffraction patterns of fluorescent aluminous oxides.
(a) ruby (Cr^{3+}/Al_2O_3), (b) $Cr^{3+}/MgAl_2O_4$, and (c) $Ce^{3+}/Y_3Al_5O_{12}$ (Cu K_α radiation).

ion (Varsanyi *et al* 1959). The excitation spectrum of this ruby powder (figure 3a) shows two broad absorptions at 406 nm and 548 nm, which are assigned to the $^4A_{2g} \rightarrow {}^4T_{1g}$ and $^4A_{2g} \rightarrow {}^4T_{2g}$ transitions of the Cr^{3+} ion respectively (Varsanyi *et al* 1959).

Formation of ruby was also confirmed by its characteristic UV-vis diffuse reflectance absorption spectrum (figure 4). The absorption bands at 402 nm and 555 nm could be assigned to the spectral transitions $^4A_{2g} \rightarrow {}^4T_{1g}$ and $^4A_{2g} \rightarrow {}^4T_{2g}$ of the Cr^{3+} ion respectively (Imbush 1978). A sharp but weak band observed at

Table 2. Properties of combustion products.

| Fluorescent oxide products	Surface area (m^2/g)	Particle size (from surface area) (μm)	50% Average agglomerate	Excitation band (nm)	Emission band (nm)	Decay time (ms)
0·05% Cr^{3+}/Al_2O_3	8·3	0·22	4·3	406, 548	695	3·6
0·05% Cr^{3+}/$MgAl_2O_4$	21·8	0·10	5·2	395, 584	687	3·95
0·05% Cr^{3+}/$LaAlO_3$	3·5	0·35	1·2	514	734	52·0
0·05% Ce^{3+}/$Y_3Al_5O_{12}$	3·3	0·47	2·2	440, 340	545	0·104
0·14% Ce^{3+}/$CaAl_{12}O_{19}$	8·5	0·25	4·1	265	325	—
$CeMgAl_{11}O_{19}$	20·2	0·15	3·2	281	370	—
0·14% Ce^{3+}/$LaMgAl_{11}O_{19}$	18·0	0·20	3·4	275	337	—
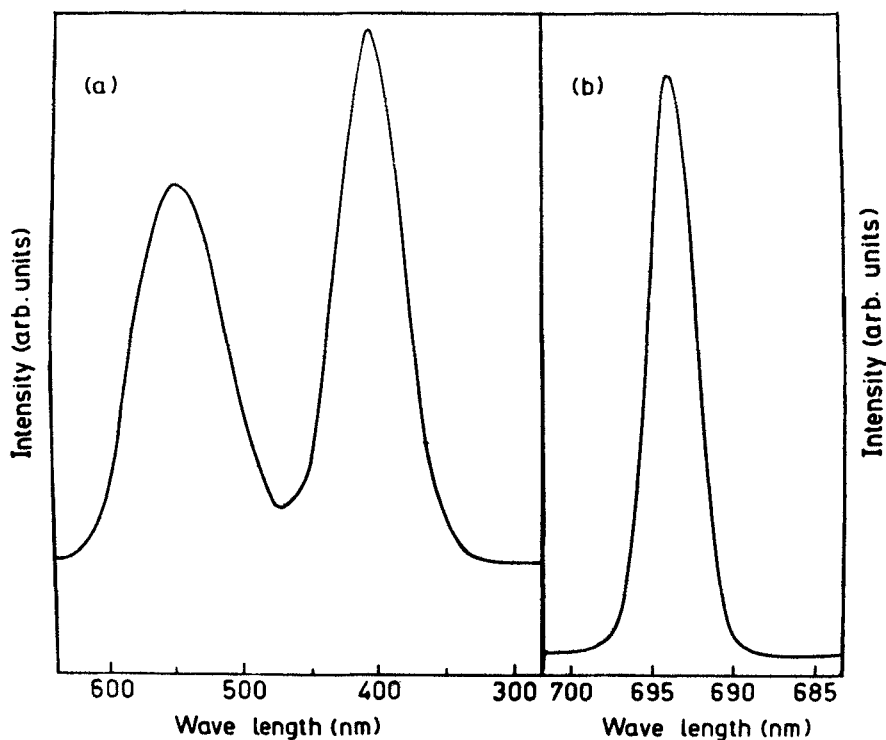
Figure 3. Fluorescence spectra of the as-prepared ruby powder: (a) excitation spectrum and (b) emission spectrum.

695 nm could be attributed (Imbush 1978) to the spin forbidden transition $^4A_{2g}$ → $^2E_{2g}$.

Formation of ruby (0·05% Cr^{3+}-doped α-Al_2O_3) powder was further confirmed by its decay time using pulsed-laser decay-time measurement. The decay curve of this powder is shown in figure 5a. It shows a characteristic decay of Cr^{3+} in the α-Al_2O_3 lattice. The decay is single exponential in nature which is further confirmed by its straight line fit in the ln (intensity) vs time plot (figure 5b). The decay time of Cr^{3+} in this powder, calculated from the slope of this ln (intensity) vs time plot, is
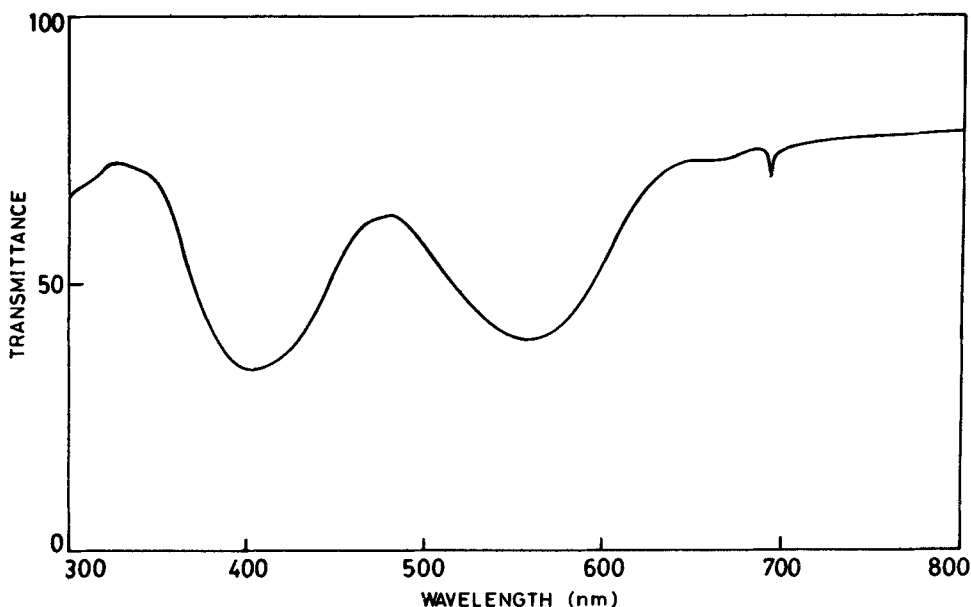
Figure 4. UV-vis diffuse reflectance absorption spectrum of the as-prepared ruby powder.

3·6 ms. This value is comparable with 4·2 ms reported in the literature for single crystal ruby at room temperature (Maiman *et al* 1961; Cronemeyer 1964; Nelson and Sturge 1965; Mahan *et al* 1969).

The presence of Cr^{3+} in Al_2O_3 was also identified by electron spin resonance (ESR) spectra of the powder. The ESR spectrum of the combustion-synthesized ruby powder (figure 6) is similar to that reported in the literature (De Biasi and Rodrigues 1985).

The combustion mixture containing higher concentrations of Cr^{3+} ions (such as the one used in the experimental section) also resulted in the formation of ruby powder having an intense pink colour and gave fluorescence spectra exactly similar to figure 3. It is worth mentioning that combustion-synthesized ruby powders with more than 2% Cr^{3+}/Al_2O_3 had traces of green colour in some portions due to the presence of unreacted Cr_2O_3. This could be due to the comparatively short period for which the high *in situ* temperatures prevail in the combustion process. It may be noted that $Cr_2O_3:Al_2O_3$ forms solid solutions in the entire range only after long heat-treatment as in metallurgical processes (Jacob 1978).

Thus it was possible to dope desired concentrations of Cr^{3+} ion (up to 2%) in α-Al_2O_3 to obtain ruby in powder form by the combustion of aluminium nitrate–urea mixtures containing chromium nitrate. Formation of homogeneous single phase ruby powder not only demonstrates the capability of the combustion process in the atomic level doping of impurity ions in the host lattices but also confirms the highly exothermic (flame temperature $\geqslant 1350°C$) nature of combustion.

3.2 *Properties of Cr^{3+}-doped $MgAl_2O_4$ and $LaAlO_3$*

The combustion process used for the preparation of ruby powder could also be

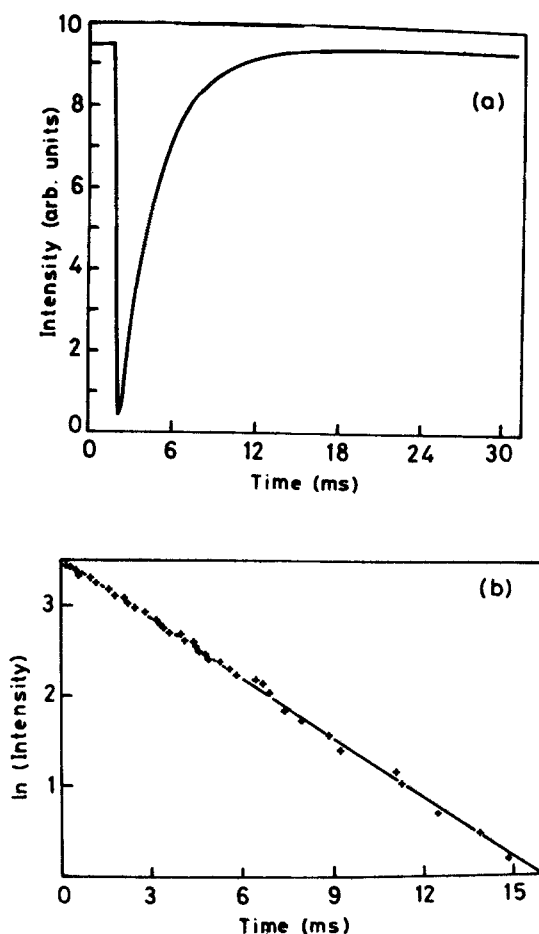**Figure 5.** (a) The decay curve of ruby powder and   (b) ln (intensity) *vs* time plot of ruby powder.

used to prepare other Cr^{3+}-doped aluminous oxides like $Cr^{3+}/MgAl_2O_4$ and $Cr^{3+}/LaAlO_3$ by the combustion of corresponding metal nitrate–aluminium nitrate–urea mixtures containing chromium nitrate. The actual compositions used for their synthesis are given in table 1. The formation of these doped oxides e.g. $Cr^{3+}/MgAl_2O_4$ have been confirmed by their characteristic pink colour, XRD (figure 2) and fluorescence spectra (Wood *et al* 1968; McCarthy and Gudel 1988). The fluorescence spectral data for these doped oxides are summarized in table 1. The fluorescence spectra of 0·05% $Cr^{3+}/MgAl_2O_4$ are shown in figures 7 and 8. The observed emission band at 687 nm and the excitation bands at 395 and 584 nm agree well with the literature values (Wood *et al* 1968).

Although all these lattices have Cr^{3+} ions in octahedral co-ordination, they show emission at different frequencies. This could be attributed to the difference in lattice pressures experienced by the Cr^{3+} ions. A similar interpretation has been given by Orgel (1957) for the difference in the spectra of Cr^{3+}-doped alum and Cr^{3+}-doped alumina (ruby).

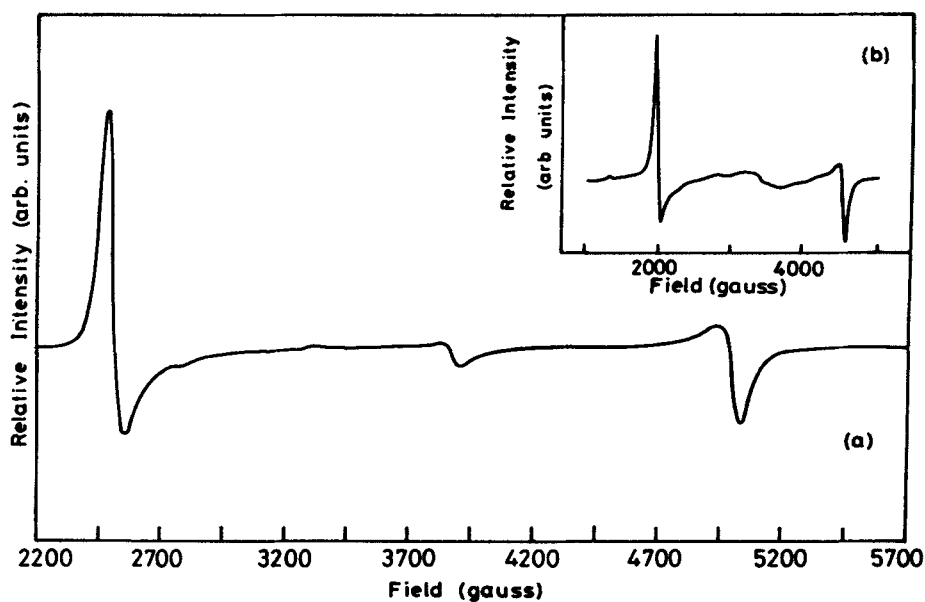**Figure 6.** The ESR spectrum of (a) the combustion synthesized ruby powder (0-05 wt.% Cr^{3+}/Al_2O_3) and (b) ruby powder (Di Biasi and Rodrigues 1985).
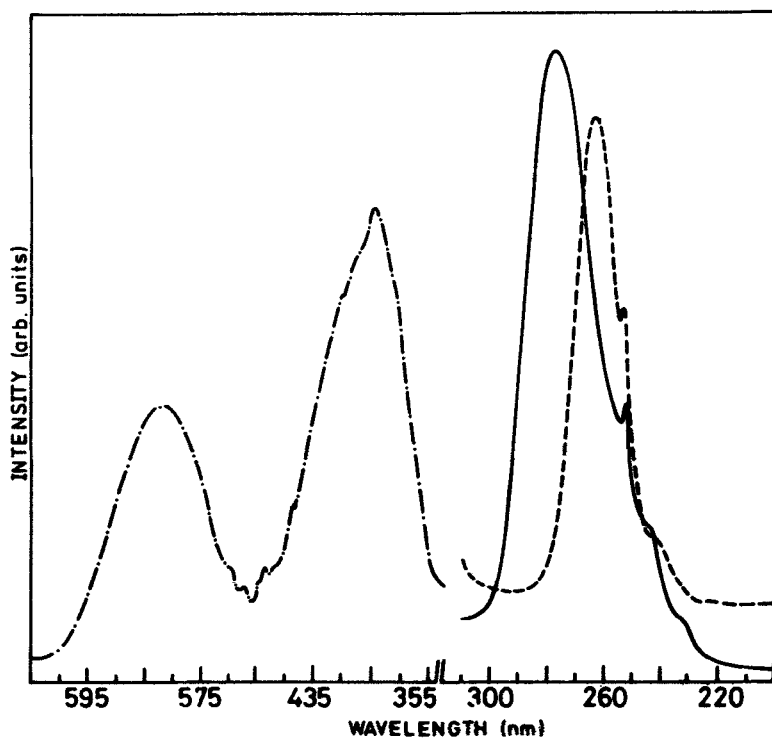

Figure 7. Excitation spectra of the fluorescence in 0-05 wt% $Cr^{3+}/MgAl_2O_4$ (—·—·—); $CaAl_{12}O_{19}:0·14\ Ce^{3+}$ (-----); $CeMgAl_{11}O_{19}$ (——).
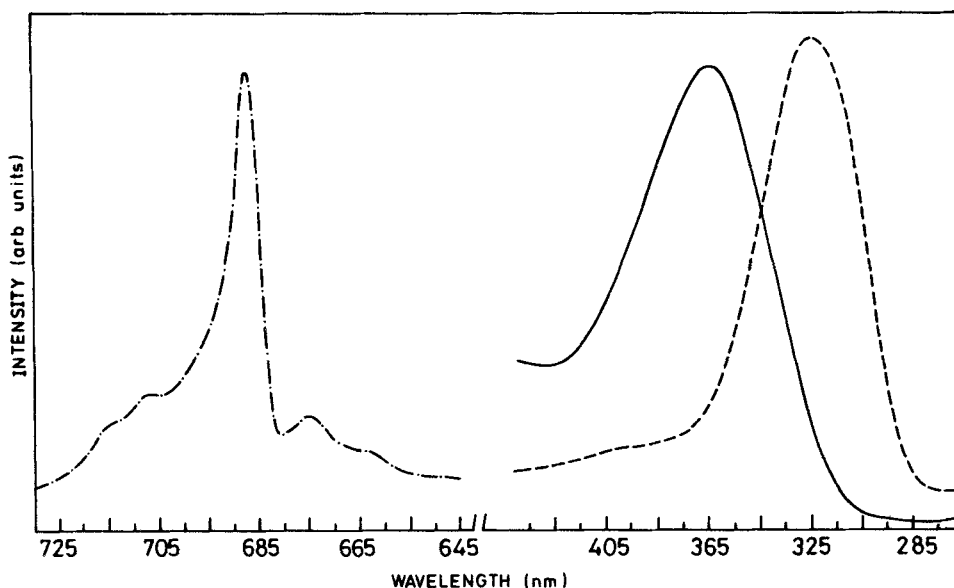
Figure 8. Emission spectra of the fluorescence in 0·05 wt% $Cr^{3+}/MgAl_2O_4$ (—·—··—); $CaAl_{12}O_{19}$:0·14 Ce^{3+} (— — —); $CeMgAl_{11}O_{19}$ (——).

The decay time values of 0·05% $Cr^{3+}/MgAl_2O_4$ and $Cr^{3+}/LaAlO_3$ are 3·9 ± 0·5 ms and 52 ± 0·5 ms respectively. $Cr^{3+}/LaAlO_3$ is of particular interest due to its longer decay time (52 ms) (slow decay). Many of the energy transfer processes are explained and well understood from the optical spectra of $Cr^{3+}/LaAlO_3$ (Siebold and Heber 1981).

3.3 *Properties of Ce^{3+}-doped aluminous oxides*

Cerium (III)-doped aluminous oxides like $Ce^{3+}/Y_3Al_5O_{12}$, $Ce^{3+}/CaAl_{12}O_{19}$, $Ce^{3+}/LaMgAl_{11}O_{19}$ and $CeMgAl_{11}O_{19}$ have been prepared by the combustion of respective metal nitrate–aluminium nitrate–urea mixtures containing $Ce(NO_3)_3·6H_2O$. The actual compositions used for their syntheses are given in table 1. Formation of these Ce^{3+}-doped oxides was confirmed by their characteristic XRD (figure 2) and fluorescence spectra. Typical fluorescence spectra of 0·14% $Ce^{3+}/CaAl_{12}O_{19}$ and $CaMgAl_{11}O_{19}$ are given in figures 7 and 8. The emission wavelengths of 0·14% $Ce^{3+}/CaAl_{12}O_{19}$ and $CeMgAl_{11}O_{19}$ are observed at 325 nm and 370 nm respectively. These results are in good agreement with the literature (Vertegan *et al* 1973; Stevels 1978). The shape of the Ce^{3+} emission band in $CeMgAl_{11}O_{19}$ is as reported (Vertegan *et al* 1973) and is similar to that of CeF_3 and $CePO_4$ (Blasse and Bril 1969).

The characteristic (Holloway and Kestigian 1967; Stevels 1978) excitation and emission wavelengths observed for 0·05% $Ce^{3+}/Y_3Al_5O_{12}$ (Holloway and Kestigian 1967) and 0·14% $Ce^{3+}/LaMgAl_{11}O_{19}$ (Stevels 1978) are given in table 2. The decay time of Ce^{3+}/YAG is 104 μs (table 2). It was interesting to observe the very bright yellow fluorescence of Ce^{3+}/YAG under the nitrogen laser during decay time measurements.

The Ce^{3+}-ion doped aluminous oxides like $Ce^{3+}/CaAl_{12}O_{19}$, Ce^{3+}/YAG and

$CeMgAl_{11}O_{19}$ are fine powders and have particle sizes of 0·2 to 0·8 μm in agglomerates sizes of 2–4 μm. These fine particle oxides are of interest for application as phosphors in TV screens and in fluorescent lamps.

4. Conclusions

Fine particles of fluorescent aluminous oxides like $Cr^{3+}/\alpha\text{-}Al_2O_3$, $Cr^{3+}/MgAl_2O_4$, $Cr^{3+}/LaAlO_3$, Cr^{3+}/YAG, Ce^{3+}/YAG, $Ce^{3+}/CaAl_{12}O_{19}$, $Ce^{3+}/LaMgAl_{11}O_{19}$ and $CeMgAl_{11}O_{19}$ have been successfully prepared by the combustion of the corresponding metal nitrate–urea/carbohydrazide mixtures at 500°C in less than 5 min. The combustion process not only yields a homogenous and stoichiometric product but also helps in atomic level substitution of impurity ions for Al^{3+} ions in the host lattice due to the high *in situ* temperatures ($> 1300°C$) that prevail during the incandescent combustion. Some fluorescent properties of these fine particle oxide materials and decay time characteristics have been studied.

References

Blasse G and Bril A 1969 *J. Chem. Phys.* **51** 3252
Cokayne B 1972 in *Modern oxide materials* (eds) B Cokayne and D W Jones (New York: Academic Press) p 1
Cronemeyer O C 1964 *J. Opt. Soc. Am.* **56** 1703
De Biasi R S and Rodrigues D C S 1981 *J. Mater. Sci.* **16** 968
De Biasi R S and Rodrigues D C S 1985 *J. Am. Ceram. Soc.* **68** 409
Geusic J E, Marcus H M and Van Uitert L G 1966 *Proc. Conf. Physics of Quantum Electronics* (New York: McGraw-Hill) p. 725
Gillen R D and Salomon R E 1970 *J. Phys. Chem.* **74** 4252
Hannay N B 1973 *XXIVth International Congress of Pure and Applied Chemistry* Vol. 3, p. 1
Hirai Y, Fukuda T, Kobayashi Y, Kuwahara H, Kido Y and Kubota K 1987 *Solid State Commun.* **62** 637
Holloway W W Jr. and Kestigian M 1967 *Phys. Lett.* **A25** 514
Imbusch G F 1978 in *Luminescence spectroscopy* (ed.) M D Lumb (New York: Academic Press) p. 1
Jacob K T 1978 *J. Electrochem. Soc.* **125** 175
Kingsley J J and Patil K C 1988 *Mater. Lett.* **6** 427–432
Kingsley J J, Sunder Manoharan S and Patil K C 1988a Ist Soviet Indian Seminar on Rare Earth and Actinide Compounds, September 19–21 Tallin, USSR
Kingsley J J, Sunder Manoharan S, Suresh K and Patil K C 1988b 2nd International Conference on Ceramic Powder Processing Science, October 12–14 (1988), Berchtesgaden, Bavaria, FRG, Deutsche Keramische Gesellschaft e.V (DKG), Abstract in: *TIZ International* 1988 **112** 726
Kingsley J J, Suresh K and Patil K C 1990 *J. Mater. Sci.* **25** 1305
Leunng K M 1986 *Phys. Rev.* **A33** 2461
Mahan A I, Bitterli C, Cannor S M and Grant D G 1969 *J. Opt. Soc. Am.* **59** 49
Maiman T H, Hoskins R H, D'Haenens I T, Asawa C K and Evtuhov V 1961 *Phys. Rev.* **123** 1151
McCarthy P J and Gudel H U 1988 *Coord. Chem. Revs.* **88** 66
Nelson D F and Sturge M D 1965 *Phys. Rev.* **A137** 1117
Orgel L F 1957 *Nature (London)* **179** 1348
Powder Diffraction File 1967 Inorganic Vol. PDIS-10, Joint Committee on Diffraction Standards, Pennsylvania
Scholten P C and Eijnthoven R 1985 Eur. Patent Appl. EP 140,448; (1985) *Chem. Abstr.* **103** 30124f
Siebold H and Heber J 1981 *J. Luminescence* **23** 325
Stevels A L N 1978 *J. Electro. Chem. Soc.* **125**
Varsanyi F, Wood D L and Schawlow A L 1959 *Phys. Rev. Lett.* **3** 544
Vertegan J M P J, Sommerdijk J L and Verriet J G 1973 *J. Luminescence* **6** 425
Wolfe W R 1978 US patent 4,088,922; (1978) *Chem. Abstr.* **89** 121750r
Wood D L, Imbusch G F, Mac Farlane R M, Kisliuk P and Larkin D M 1968 *J. Chem. Phys.* **48** 5255